J. Biochem. **136**, 39–47 (2004)
DOI: 10.1093/jb/mvh090

Fluorescence Resonance Energy Transfer between Points on Actin and the C-Terminal Region of Tropomyosin in Skeletal Muscle Thin Filaments

Masao Miki[1,*], Hong Hai[1], Kimiko Saeki[2], Yuji Shitaka[1], Ken-Ichi Sano[3], Yuichiro Maéda[3] and Takeyuki Wakabayashi[4]

[1]Department of Applied Chemistry and Biotechnology, Fukui University, 3-9-1 Bunkyo, Fukui 910-8507; [2]Department of Physics, School of Science, University of Tokyo, Hongo 7-3-1, Bunkyo-ku, Tokyo 113-0033; [3]Riken Harima Institute at Spring8, Mikazuki-cho, Sayo, Hyogo 679-5143; [4]Department of Biosciences, School of Science and Engineering, Teikyo University, Toyosatodai 1-1, Utsunomiya 320-8551

Received March 22, 2004; accepted April 22, 2004

Fluorescence resonance energy transfer between points on tropomyosin (positions 87 and 190) and actin (Gln-41, Lys-61, Cys-374, and the ATP-binding site) showed no positional change of tropomyosin relative to actin on the thin filament in response to changes in Ca^{2+} concentration (Miki *et al.* (1998) *J. Biochem.* 123, 1104–1111). This is consistent with recent electron cryo-microscopy analysis, which showed that the C-terminal one-third of tropomyosin shifted significantly towards the outer domain of actin, while the N-terminal half of tropomyosin shifted only a little (Narita *et al.* (2001) *J. Mol. Biol.* 308, 241–261). In order to detect any significant positional change of the C-terminal region of tropomyosin relative to actin, we generated mutant tropomyosin molecules with a unique cysteine residue at position 237, 245, 247, or 252 in the C-terminal region. The energy donor probe was attached to these positions on tropomyosin and the acceptor probe was attached to Cys-374 or Gln-41 of actin. These probe-labeled mutant tropomyosin molecules retain the ability to regulate the acto-S1 ATPase activity in conjunction with troponin and Ca^{2+}. Fluorescence resonance energy transfer between these points of tropomyosin and actin showed a high transfer efficiency, which should be very sensitive to changes in distance between probes attached to actin and tropomyosin. However, the transfer efficiency did not change appreciably upon removal of Ca^{2+} ions, suggesting that the C-terminal region of tropomyosin did not shift significantly relative to actin on the reconstituted thin filament in response to the change of Ca^{2+} concentration.

Key words: FRET, skeletal muscle regulation, steric blocking theory, thin filament, tropomyosin movement.

Abbreviations: 3D-EM, three-dimensional image reconstruction of electron micrographs; DABMI, 4-dimethylaminophenylazophenyl 4′-maleimide; DTT, dithiothreitol; FLC, fluorescein cadaverine; FRET, fluorescence resonance energy transfer; IAEDANS, 5-(2-iodoacetylaminoethyl)aminonaphthalene 1-sulfonic acid; S1, myosin subfragment 1; Tm, tropomyosin; Tn, troponin; TnC, troponin C; TnI, troponin I; TnT, troponin T.

In striated muscle, the interaction of myosin with actin is regulated by tropomyosin (Tm) and troponin (Tn) on actin filaments in response to a change in Ca^{2+} concentration from approximately 10^{-7} to 10^{-5} M (*1*). Tm, an extended coiled-coil dimer, binds end-to-end along the actin filament and covers seven actin monomers (*2*). Tn is a complex of three proteins: troponin C (TnC), troponin I (TnI), and troponin T (TnT). TnC, TnI and the COOH terminal region of TnT form a globular portion of Tn and are located near Cys-190 of Tm. The elongated NH_2 terminal region of TnT extends along the COOH terminal region of Tm to the beginning of the next Tm on the actin filament. Although numerous studies have characterized the interaction between the thin filament proteins to deduce how the Ca^{2+}-triggering signal is propagated from TnC to the rest of the thin filament (*3–5*), the mechanism of this regulatory process is still not well understood.

The most commonly quoted molecular interpretation of this regulatory mechanism is a steric blocking model in which, in the absence of calcium, tropomyosin physically blocks the myosin binding site on actin (*6*, *7*). According to the model, the binding of calcium to troponin causes a conformational change in the thin filament, which results in tropomyosin moving over the surface of actin to a non-blocking position. On the other hand, kinetic measurements indicated a three-state model for regulation (blocked, closed, and open) (*8–10*). The equilibrium between the blocked and closed states is Ca^{2+}-sensitive, and strong S1 binding is required in order to switch the thin filament completely into the open state. X-ray diffraction data of skinned fibers or oriented filaments and 3D-EM data of isolated thin filaments have been interpreted to indicate three positions of Tm corresponding to the three-state model (*11*, *12*). This interpretation sup-

*To whom correspondence should be addressed. Tel: +81-776-27-8786, Fax: +81-776-27-8747, E-mail: masao@acbio2.acbio.fukui-u.ac.jp

ports a steric blocking model in which Tm blocks the myosin-binding site by changing its positions on the actin filament. However, the Ca^{2+}-induced conformational change of the thin filament cannot clearly be assigned to the movement of Tm from these data, since this interpretation is based on the assumption that the mass of Tn/Tm complex is distributed evenly and smoothly all through the continuous Tm strands. Narita *et al*. (*13*) analyzed the data of 3D-EM without imposing helical symmetry in the reconstruction of the three-dimensional structure of a thin filament. They concluded that during inhibition, tropomyosin shifted differentially: the N-terminal half of Tm shifted only slightly but the C-terminal one-third of Tm and/or Tn tail shifted significantly towards the outer domain of actin.

Fluorescence resonance energy transfer (FRET) is a powerful method to detect a change in the distance between fluorescent probes attached to a protein, because the transfer efficiency is a function of the inverse of the sixth power of the distance between probes (*14*, *15*). However, for application of this method, the attachment of a probe at a very specific position on protein is critical. Recent progress in genetic engineering has made this method more powerful, since the selective labeling of protein at an appropriate position is made easier by use of a single cysteine mutant protein. Several attempts to detect a positional change of Tm or Tn on actin have been made (*16–27*). FRET between probes attached to TnI (at positions 9, 117, and 133) or TnT (at positions 60, and 250) and actin (at positions Gln-41 and Cys-374) demonstrated a significant Ca^{2+}- or S1-induced movement of TnI and TnT (*25–27*). However, FRET between probes on Tm (at positions 87 and 190) and actin (at positions Gln-41, Lys-61, Cys-374, and the nucleotide-binding site) did not show any significant Ca^{2+}- or S1-induced movement of Tm (*16–18*, *22*, *23*, *25*). Because residues 87 and 190 of Tm are located in its N-terminal region, the FRET results are consistent with the results of Narita *et al*. (*13*), which showed almost no Ca^{2+}-induced shift of Tm in this region. But they did observe the Ca^{2+}-induced shift of the C-terminal one-third of Tm and/or Tn tail. We therefore generated several mutant Tms in which the amino acid residue at position 237, 245, 247, or 252 in the C-terminal one-third was replaced with single cysteine for use as a donor-labeling site. In the present study, FRET between probes attached to these sites on Tm and actin was measured to detect a Ca^{2+}- or S1-induced movement of Tm.

MATERIALS AND METHODS

Reagents—Phalloidin from *Amanita phalloides* was purchased from Sigma Chemical Co. IAEDANS, DABMI and FLC were from Molecular Probes. BCA protein assay reagent was from Pierce Chemicals. All other chemicals were of analytical grade.

Protein Preparations—Actin, S1, and troponin from rabbit skeletal muscle were prepared as described in a previous report (*18*). α-Tm was extracted from rabbit hearts as previously reported (*18*). Microbial transglutaminase was a generous gift from the Food Research and Development Laboratories, Ajinomoto Co. Unlike transglutaminase from guinea pigs, this enzyme does not require Ca^{2+} for its activity (*28*, *29*).

Preparation of Mutant Tm—A plasmid containing a cDNA clone of the rabbit α-tropomyosin gene was kindly provided by Dr. K. Maeda (*30*). The plasmid construction was modified using the polymerase chain reaction (PCR). The N-terminal primer was 5′-ccccatatggcggcgagcatggacgccatcaagaagaagat (*Nde*I site underlined) and the C-terminal primer was 5′-cgcgtcgacttatatggaagtcatatcgttgagag (*Sal*I site underlined). The PCR product was cloned into pET24a+ (Novagen Inc.) using *Nde*I and *Sal*I sites. This construct (pET-AASTm) was expected to express a recombinant tropomyosin with an additional N-terminal Ala-Ala-Ser. This tripeptide added at the N-terminus of recombinant tropomyosin can perform the function of the N-acetyl group present on muscle tropomyosin (*31*). Expression plasmids containing mutation C190I, C190I/T237C, C190I/S245C, C190I/ T247C, and C190I/ S252C were constituted by oligonucleotide-directed mutagenesis (*32*). Expression in *E. coli* and purification of expressed AASTm were carried out according to Kluwe *et. al.* (*30*) and Miegel *et. al*. (*33*) respectively.

The expression vector for rabbit skeletal muscle β-tropomyosin was constructed as follows. PCR was carried out to add the extra Ala-Ala-Ser sequence at the N-terminal of the expressed protein and to generate one *Nde*I and one *Bam*HI site. The sequences of PCR primers were: 5′-gggcatatggcggcgtcgatggacgccatcaagaagaag-3′ and 5′-gggggatccttagagggaagtgatgtcgttgagcg-3′, and a cDNA library from skeletal muscle (Stratagene) was used as a template. The PCR product was digested with *Nde*I and *Bam*HI and inserted into the corresponding sites of pET3a.

Labeling of Proteins—Actin was labeled at Cys-374 with DABMI or at Gln-41 with FLC as previously reported (*18*, *21*). Wild-type αα-Tm was labeled at Cys-190 and αα-mTm at Cys-237, 245, 247 or 252 with IAEDANS as previously reported (*18*, *22*). The absorption coefficients of 24,800 M^{-1} cm^{-1} at 460 nm for DABMI (*17*), 75,500 M^{-1} cm^{-1} at 493 nm for FLC (*34*), and 6,100 M^{-1} cm^{-1} at 337 nm for IAEDANS (*35*) were used for the determination of the labeling ratios. The labeling ratios were 0.83 for FLC to actin, 1.0 for DABMI to actin, and 1.31, 1.12, 1.62, or 1.67 for AEDANS to mutant αα-Tm at Cys-237, Cys-245, Cys-247, or Cys-252, respectively. The heterodimer αβ-mTm singly labeled with IAEDANS was prepared according to the method of Graceffa (*36*, *37*). αα-mTm labeled with IAEDANS at Cys-237, 245, 247 or 252 was combined with unlabeled ββ-Tm at an αα/ββ molar ratio of 1.15, incubated at 50°C to dissociate all dimers into single chains, and then re-associated as a heterodimer by slowly cooling down.

Spectroscopic Measurements—Absorption was measured with a Hitachi U2000 spectrophotometer. The following extinction coefficients were used to calculate protein concentrations: $A_{290\ nm}$ = 0.63 $(mg/ml)^{-1}$ cm^{-1} for G-actin, and $A_{280\ nm}$ = 0.75 for S1, 0.33 for Tm, and 0.45 $(mg/ml)^{-1}$ cm^{-1} for Tn. Concentrations of labeled proteins and transglutaminase were measured with the Pierce BCA protein assay reagent. Relative molecular masses of 42,000 for actin, 115,000 for S1, 66,000 for Tm, 69,000 for Tn, and 38,000 for microbial transglutaminase were used. Steady-state fluorescence was measured at 20°C

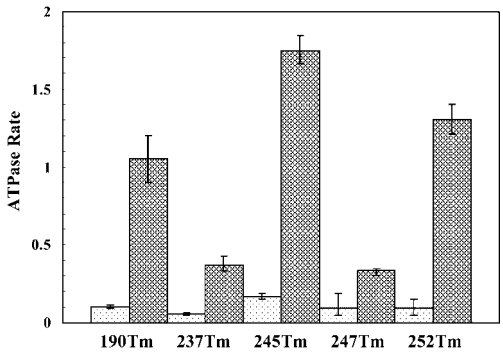

Fig. 1. **Regulation of acto-S1 ATPase by various IAEDANS-labeled mutant tropomyosins.** 190Tm is the rabbit skeletal ααTm which has a unique cysteine at position 190. 237Tm, 245Tm, 247Tm, or 252Tm is a mutant Tm which has a unique cysteine at position 237, 245, 247, or 252, respectively. The ATPase rate of acto-S1 without troponin-tropomyosin is normalized as 1.0. Acto-S1 ATPase activity was measured at 25°C in 10 mM KCl, 5 mM $MgCl_2$, 2 mM ATP, 20 mM Tris–HCl (PH7.6), and 1 mM DTT, with 50 μM $CaCl_2$ (+Ca^{2+}; striped bar) or 1 mM EGTA (–Ca^{2+}; dotted bar). Protein concentrations were 4 μM F-actin, 1 μM S1, 0.57 μM Tm, and 0.67 μM Tn. Error bars indicate standard deviations (n = 4).

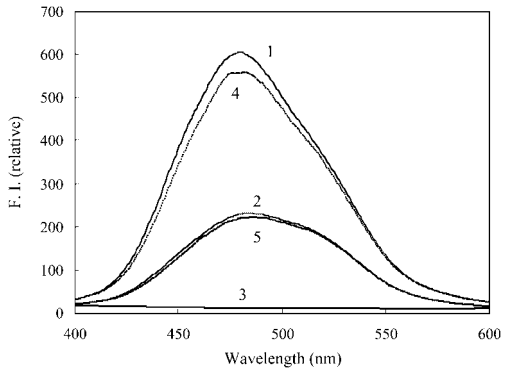

Fig. 2. **Fluorescence spectra of AEDANS bound to Cys-252 of mTm on reconstituted thin filaments in the presence and absence of an acceptor (DABMI bound to Cys-374 of actin).** (1) F-actin/Tn/AEDANS-mTm/+Ca^{2+}, (2) DABMI-F-actin/Tn/AEDANS-mTm/+Ca^{2+}, (3) DABMI-F-actin/Tn/mTm/±Ca^{2+}, (4) F-actin/Tn/AEDANS-mTm/–Ca^{2+}, (5) DABMI-F-actin/Tn/AEDANS-mTm/–Ca^{2+}. Spectra were measured at 20 °C in 30 mM KCl, 2 mM $MgCl_2$, 20 mM Tris-HCl (pH 7.6), 0.1 mM ATP, 1 mM NaN_3 (buffer F), and 50 μM $CaCl_2$ for the +Ca^{2+} state or 1 mM EGTA for the –Ca^{2+} state. The concentrations of actin, Tm and Tn were 0.2, 0.044, and 0.046 mg/ml, respectively. Excitation was at 340 nm.

with a Perkin Elmer LS50B fluorometer. Sample cells were placed in a thermostated cell holder. Stopped flow experiments were performed using an Applied Photophysics stopped-flow spectrofluorometer SX.18MV. The dead time of the stopped-flow apparatus was 1.4 ms.

Fluorescence Resonance Energy Transfer—The efficiency E of resonance energy transfer between probes was determined by measuring the fluorescence intensity of the donor both in the presence (F_{DA}) and absence (F_{D0}) of the acceptor, as given by

$$E = 1 - F_{DA}/F_{D0} \quad (1)$$

The efficiency is related to the distance (R) between donor and acceptor and to Förster's critical distance (R_0) at which the transfer efficiency is equal to 50%

$$E = R_0^6/(R^6 + R_0^6) \quad (2)$$

R_0 can be obtained (in nm) from:

$$R_0^6 = (8.79 \times 10^{-11})\, n^{-4}\, \kappa^2\, Q_0 J \quad (3)$$

where n is the refractive index of the medium taken as 1.4, κ^2 is the orientation factor, Q_0 is the quantum yield of the donor in the absence of the acceptor, and J is the spectral overlap integral between the donor emission $F_D(\lambda)$ and acceptor absorption $\varepsilon_A(\lambda)$ spectra, defined by

$$J = \int F_D(\lambda)\, \varepsilon_A(\lambda)\, \lambda^4\, d\lambda / \int F_D(\lambda)\, d\lambda \quad (4)$$

The quantum yield was determined by a comparative method using quinine sulfate in 1 M H_2SO_4 as the standard, which has an absolute quantum yield of 0.70 (*38*). The value of κ^2 was taken as 2/3 for calculation of distances both in the presence and absence of Ca^{2+} and/or S1, as mentioned previously (*14*). The decrease of the fluorescence intensity due to inner filter effects was corrected with

$$F_{corr} = F_{obs} \times 10^{(Aex + Aem)/2} \quad (5)$$

where A_{ex} and A_{em} are absorption of the sample at the excitation and emission wavelengths, respectively.

Other Methods—SDS-PAGE was carried out according to Laemmli (*39*). ATPase activity was measured by the method of Tausky and Shorr (*40*).

RESULTS

Regulation of the Acto-S1 ATPase by mutant Tm—In this work, the AEDANS moiety bound at the position of 237, 245, 247, or 252 on mutant Tm was used as the energy-transfer donor, while FLC or DABMI bound to Gln-41 or Cys-374 in F-actin respectively, was used as the energy-transfer acceptor. To test whether the labeled mutant Tm retains the essential property of being able to participate in the calcium regulation process, the ATPase activities of reconstituted systems composed of S1, Tn, Tm, and F-actin were measured in the presence and absence of Ca^{2+}. Measurements were performed at 25°C in 10 mM KCl, 5 mM $MgCl_2$, 2.0 mM ATP, 20 mM Tris–HCl (pH 7.6), 1 mM DTT, and 50 μM $CaCl_2$ (+Ca^{2+} state) or 1 mM EGTA (–Ca^{2+} state). Protein concentrations were 4 μM F-actin, 0.57 μM Tm, 0.67 μM Tn and 1 μM S1. Figure 1 shows the ability of the labeled mutant Tm to regulate the myosin S1-ATPase in the presence of Tn, either with or without Ca^{2+}. The ATPase activity of actoS1 in the absence of regulatory proteins was taken to be 1.0 for reference. Compared with wild-type Tm, the reconstituted system with AEDANS-labeled mTm (S245C) or mTm (S252C) showed higher activity, while labeled mTm (T237C) and mTm (T247C) showed lower activities in the presence of Ca^{2+}. On the other hand, in the absence of Ca^{2+}, the ATPase activity was significantly

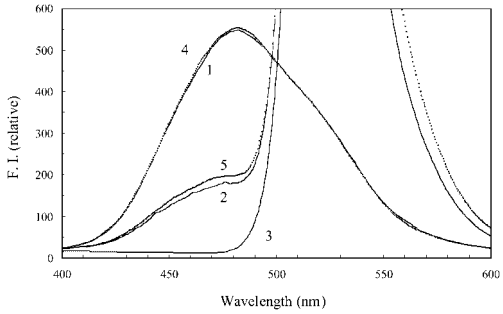

Fig. 3. **Fluorescence spectra of AEDANS bound to Cys-247 of mTm on reconstituted thin filaments in the presence and absence of an acceptor (FLC bound to Gln-41 of actin).** (1) F-actin/Tn/AEDANS-mTm/+Ca^{2+}, (2) FLC-F-actin/Tn/AEDANS-mTm/+Ca^{2+}, (3) FLC-F-actin/Tn/mTm/±Ca^{2+}, (4) F-actin/Tn/AEDANS-mTm/–Ca^{2+}, (5) FLC-F-actin/Tn/AEDANS-mTm/–Ca^{2+}. Spectra were measured under the same conditions as in Fig. 2.

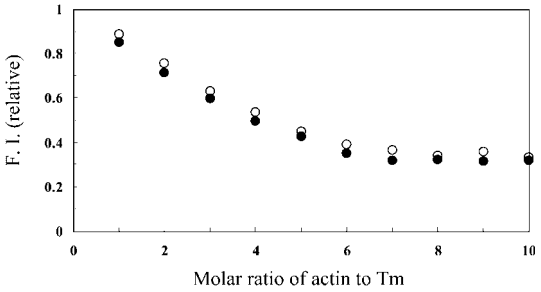

Fig. 4. **Relative fluorescence intensities of AEDANS bound to Cys-237 of mTm on reconstituted thin filaments *vs.* molar ratio of DABMI-F-actin to Tm in the presence (solid circles) and absence (open circles) of Ca^{2+}.** Excitation was at 340 nm and emission was measured at 490 nm. Values were obtained in buffer F with 50 μM $CaCl_2$ for the +Ca^{2+} state or 1 mM EGTA for the –Ca^{2+} state at 20°C, after correction of the inner filter effects according to Eq. 5. The concentrations of Tm and Tn were 0.044 and 0.046 mg/ml, respectively.

reduced for all labeled mTms. The regulatory capacity value is defined as 1 – (Act_{-Ca}/Act_{+Ca}), where Act_{-Ca} and Act_{+Ca} are the Mg-ATPase activities in the absence and presence of Ca^{2+}, respectively. The values for wild-type Tm, labeled mTm (T237C), mTm (S245C), mTm (T247C), and mTm (S252C) were 0.89, 0.89, 0.89, 0.86, and 0.96, respectively. The results showed that the AEDANS-labeled mutant Tms retain their essential properties, being able to participate in the calcium regulation process.

FRET between Probes Attached to mTm and Actin on Reconstituted Thin Filaments in the Presence and Absence of Ca^{2+}—Figure 2 shows the fluorescence spectra of AEDANS-252-mTm on reconstituted thin filaments in the presence (curves 2 and 5) and absence (curves 1 and 4) of an acceptor (DABMI bound to F-actin). The solvent conditions were 30 mM KCl, 20 mM Tris–HCl (pH 7.6), 2 mM $MgCl_2$, 0.1 mM ATP, and 1 mM NaN_3 (buffer F) with 50 μM $CaCl_2$ for the +Ca^{2+} state (curves 1 and 2) or 1 mM EGTA for the –Ca^{2+} state (curves 4 and 5) at 20°C. Spectra show that the donor fluorescence was quenched by ~60% in the presence of the acceptor due to energy transfer, and the transfer efficiency in this range should be very sensitive to a distance change. The intensity of the donor fluorescence on Tm was smaller for the –Ca^{2+} state than for the +Ca^{2+} state, but the ratio of donor fluorescence in the presence of acceptor to that in the absence of acceptor was not sensitive to Ca^{2+} concentration. This result suggests that the probe on Tm does not significantly change its position on the actin filament with changes in Ca^{2+} concentration.

Figure 3 shows the fluorescence spectra of AEDANS-247-mTm on reconstituted thin filaments in the presence (curves 2 and 5) and absence (curves 1 and 4) of an acceptor (FLC bound to F-actin) for +Ca^{2+} state (curves 1 and 2) or for –Ca^{2+} state (curves 4 and 5) at 20°C. The donor fluorescence was significantly quenched in the presence of the acceptor at wavelengths shorter than 480 nm. This can be attributed mainly to resonance energy transfer from AEDANS-mTm to FLC-F-actin. The ratio of donor fluorescence in the presence of acceptor to that in the absence of acceptor was not sensitive to Ca^{2+} concentration.

Titration of Tn-Tm with DABMI-Actin—To obtain more quantitative data on the transfer efficiency, the ratio of the donor quenching was measured by titrating AEDANS-mTm/Tn with DAB-F-actin in the presence (buffer F + 50 μM $CaCl_2$) or absence of Ca^{2+} ions (buffer F + 1 mM EGTA) at 20°C. The fluorescence intensity was measured at 490 nm. Figure 4 shows the case of AEDANS-237-mTm and DAB-F-actin. For correction of the fluorescence intensity change of AEDANS-mTm upon binding to an actin filament, the same amount of non-labeled F-actin was added to AEDANS-mTm/Tn as a reference, and the ratio of these fluorescence intensities was taken as the relative fluorescence intensity. The apparent decrease in the fluorescence intensity due to inner filter effects arising from the absorbance of DAB-F-actin was corrected according to Eq. 5. The relative fluorescence intensity decreased gradually in the actin/Tm molar ratio range up to 7 and became almost constant in the range over 7. From the saturation points, the transfer efficiency was calculated for the +Ca^{2+} and –Ca^{2+} states. The transfer efficiencies for other mutant Tms were obtained in the same way, and the results are summarized in Table 1. In all cases, there was no significant difference in the extent

Table 1. **Distances between probes attached to *aa*-mTm and actin (Cys-374) in reconstituted thin filaments in the presence and absence of Ca^{2+} ions.**

mTm	Q_0	J ($\times 10^{14}$ nm^4 M^{-1} cm^{-1}) (Cys-374 of actin)	R_0 (Å)	E (+Ca^{2+}/–Ca^{2+})	R (2/3) (Å) (+Ca^{2+}/–Ca^{2+})
252	0.36	6.62	39.2	0.54 ± 0.02/0.51 ± 0.03	38.2 ± 0.5/38.9 ± 0.8
247	0.29	6.53	37.7	0.58 ± 0.03/0.58 ± 0.02	35.7 ± 0.7/35.7 ± 0.5
245	0.29	6.60	37.8	0.57 ± 0.01/0.58 ± 0.02	36.1 ± 0.2/35.8 ± 0.5
237	0.31	6.81	38.4	0.68 ± 0.01/0.65 ± 0.02	33.9 ± 0.3/34.6 ± 0.5

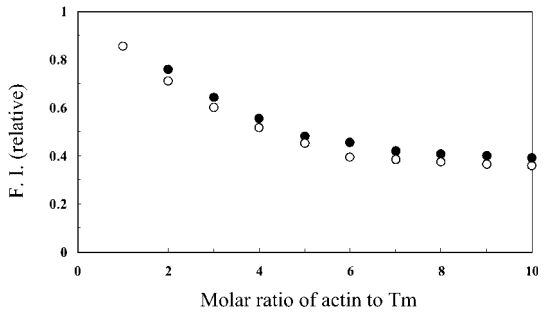

Fig. 5. **Relative fluorescence intensities of AEDANS bound to Cys-247 of mTm on reconstituted thin filaments *vs.* molar ratio of FLC-F-actin to Tm in the presence (solid cirlces) and absence (open circles) of Ca^{2+}.** Excitation was at 340 nm and emission was measured at 460 nm. Values were obtained as in Fig. 4.

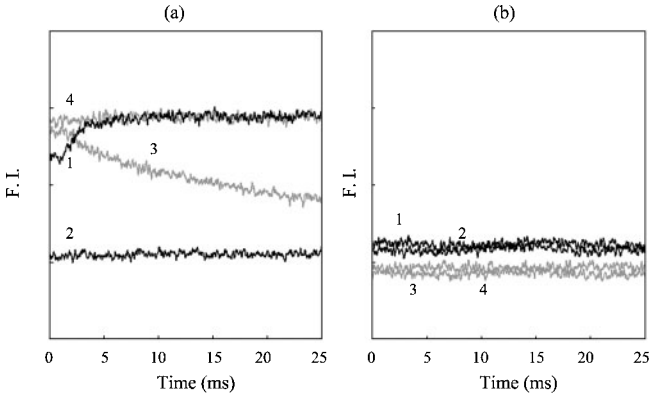

Fig. 6. **Kinetic tracing of the stopped-flow experiments.** (a) A solution of 4.8 μM DABMI-F-actin, 0.66 μM Tm, and 0.66 μM AEDANS-Tn in buffer F/3.75 mM EGTA was mixed with an equal volume of buffer F containing 4 mM $CaCl_2$ (1; $-Ca^{2+} \rightarrow +Ca^{2+}$) or 3.75 mM EGTA (2; $-Ca^{2+} \rightarrow -Ca^{2+}$) at 20°C. DABMI-FA/Tm/AEDANS-Tn in buffer F/0.1 mM $CaCl_2$ was mixed with an equal volume of buffer F containing 3.75 mM EGTA (3; $+Ca^{2+} \rightarrow -Ca^{2+}$) or 0.1 mM $CaCl_2$ (4; $+Ca^{2+} \rightarrow +Ca^{2+}$). The excitation wavelength was 340 nm, and emission from 420 to 540 nm was collected by use of a broad band cut filter (Chroma Technology Co.). (b) A solution of 4.8 μM DABMI-F-actin, 0.66 μM AEDANS-Tm, and 0.66 μM Tn in buffer F was measured under the same conditions as in (a).

of the transfer efficiency between the $+Ca^{2+}$ and $-Ca^{2+}$ states.

Titration of Tn-Tm with FLC-Actin—The AEDANS-247-mTm/Tn was also titrated with FLC-F-actin in the presence or absence of Ca^{2+} ions in the same way as the case of DAB-F-actin. Fluorescence intensity was measured at 460 nm, at which wavelength FLC makes no contribution to the acceptor-fluorescence, as can be seen in Fig. 3. The titration showed almost the same curves as the case of DAB-F-actin (Fig. 5). From the saturation points, the transfer efficiencies were calculated to be 0.75 ± 0.05 for $\pm Ca^{2+}$ states, corresponding to the distance of 36.6 Å. There was no difference between $+Ca^{2+}$ and $-Ca^{2+}$ states. The transfer efficiencies for other mutant Tms were obtained in the same way and the results are summarized in Table 2.

The αβ mTm Singly Labeled at Cys-237, 245, 247, or 252 with IAEDANS—Graceffa (*37*) suggested the possibility that ααTm has a donor symmetrically protruding from either side of the Tm coiled-coil, and that such a broad donor on Tm may lower the sensitivity of FRET efficiency to a distance change deriving from Tm movement on an F-actin filament. Then, heterodimers singly labeled at Cys-237, 245, 247, or 252 with IAEDANS were prepared according to the method of Graceffa (*37*). FRET measurements between IAEDANS attached to the singly labeled heterodimer αβ mTm and DABMI attached to Cys-374 of actin on reconstituted thin filaments were carried out by the same experimental procedures as the case of homodimer αα mTm. By titrating AEDANS-αβ mTm with DABMI-F-actin in the presence or absence of Ca^{2+} ions, the transfer efficiencies were obtained. The results are summarized in Table 3. The calculated distances R (2/3) are not sensitive to Ca^{2+} concentration. Furthermore, there was no substantial difference in the calculated distances (2/3) between homodimer αα mTm and heterodimer αβ mTm. Therefore, it seems unlikely that the heterodimer αβ mTm binds to itself end-to-end on actin such that the α chain is always on the same side of the Tm polymer.

Stopped-Flow Measurements—FRET in combination with stopped-flow methods showed that, after the bind-

Table 2. **Distances between probes attached to *αα*-mTm and actin (Gln-41) in reconstituted thin filaments in the presence and absence of Ca^{2+} ions.**

mTm (αα)	Q_0	J ($\times 10^{14}$ nm^4 M^{-1} cm^{-1}) (Gln-41 of actin)	R_0 (Å)	E ($+Ca^{2+}/-Ca^{2+}$)	R (2/3) (Å) ($+Ca^{2+}/-Ca^{2+}$)
252	0.36	16.49	45.7	0.73 ± 0.03/0.62 ± 0.04	38.7 ± 1.0/42.1 ± 1.2
247	0.29	16.51	44.0	0.75 ± 0.05/0.75 ± 0.05	36.6 ± 1.7/36.6 ± 1.7
245	0.29	16.40	44.0	0.76 ± 0.05/0.73 ± 0.02	36.3 ± 1.8/37.3 ± 0.6
237	0.31	16.73	44.6	0.88 ± 0.01/0.85 ± 0.01	32.0 ± 0.5/33.4 ± 0.4

Table 3. **Distances between probes attached to *αβ*-mTm and actin (Cys-374) in reconstituted thin filaments in the presence and absence of Ca^{2+} ions.**

mTm (αβ)	Q_0	J ($\times 10^{14}$ nm^4 M^{-1} cm^{-1}) (Cys-374 of actin)	R_0 (Å)	E ($+Ca^{2+}/-Ca^{2+}$)	R (2/3) (Å) ($+Ca^{2+}/-Ca^{2+}$)
252	0.35	6.69	39.1	0.54 ± 0.02/0.49 ± 0.04	38.1 ± 0.5/39.4 ± 1.1
247	0.30	6.67	38.1	0.58 ± 0.03/0.55 ± 0.06	36.1 ± 0.7/36.8 ± 1.5
245	0.28	6.67	37.7	0.55 ± 0.01/0.56 ± 0.01	36.5 ± 0.2/36.2 ± 0.2
237	0.31	7.13	38.7	0.68 ± 0.01/0.66 ± 0.01	34.1 ± 0.3/34.6 ± 0.3

ing of Ca^{2+} to TnC, TnI detached from the outer domain of actin on the thin filament with a time scale of several milliseconds (*20*). In the present study, the donor molecule, IAEDANS, was attached to Cys-133 of TnI, and the acceptor molecule, DABMI, was attached to Cys374 of actin. Figure 6 (a) shows the time courses of fluorescence intensity change of AEDANS-Tn in reconstituted thin filaments followed by stopped-flow measurements after changing the solvent conditions from $-Ca^{2+}$ to $+Ca^{2+}$ or vice versa. On the transition from $-Ca^{2+}$ to $+Ca^{2+}$ solvent conditions, the fluorescence intensity increased very rapidly and reached a final fluorescence level at around 10 ms after the flow-stop point. The rate constant was calculated as $569 \pm 100\ s^{-1}$. On the other hand, on the transition from $+Ca^{2+}$ to $-Ca^{2+}$, the fluorescence intensity decreased with a much slower rate constant of $83.6 \pm 1.2\ s^{-1}$. These rate constants are almost the same as previously reported (*20*). Steady-state FRET measurements between points on actin and Tm did not show any significant change in the transfer efficiency with changes in Ca^{2+} concentration. Even though an azimuthal movement of Tm on an actin filament does not produce any distance change between the donor on Tm and the acceptor on actin after the completion of the movement, during the movement of Tm, the distance might change substantially. It is reasonable to assume that the proposed movement of Tm should be simultaneous with or later than the movement of TnI. Therefore, when the transition is followed by time-resolved FRET using the stopped-flow method, some trace of Tm movement should be detectable after TnI movement. The donor molecule, IAEDANS, was attached to Cys190 of $\alpha\alpha$Tm and the acceptor molecule, DABMI was attached to Cys-374 of actin. Figure 6 (b) shows the time courses of fluorescence intensity change of AEDANS-Tm in reconstituted thin filaments followed by stopped-flow measurements after changing the solvent conditions from $-Ca^{2+}$ to $+Ca^{2+}$ or vice versa. In contrast to the case of AEDANS-Tn, the fluorescence intensity of AEDANS-Tm did not change appreciably. This suggests that there is no intermediate position of the probe attached to Tm on an F-actin filament during the transition from $+Ca^{2+}$ to $-Ca^{2+}$, even if Tm changes its position. Thus, FRET changes due to the proposed Tm movement could not be detected.

DISCUSSION

Since a steric blocking model was proposed more than a quarter century ago from low angle X-ray scattering measurements (*6*, *7*), this model has been widely accepted because it provides a simple image for regulation mechanism of muscle contraction. In this model, the azimuthal movement of Tm on actin filaments is a critical event for blocking the myosin-binding site. Since then, numerous structural studies using low angle X-ray scattering and 3D-EM have indicated that conformational changes of thin filaments could be explained as Tm movement on actin filaments (see review *5*). However, the interpretation of these measurements has been questioned because they do not take into consideration the presence of Tn and possible changes in its structure with Ca^{2+}, although Tn is rather larger in mass than Tm. Squire and Morris (*41*) suggested that conformational changes observed from X-ray diffraction data could be explained as Tn movement instead of Tm movement. Narita *et al*. reconstructed three-dimensional images of thin filaments from electron cryo-micrographs without imposing helical symmetry and showed that troponin does move (*13*). They showed that the major change due to Ca^{2+} is the shift of Tn head (main body of Tn), and that the N-terminal half of Tm does not shift much but the C-terminal one-third of Tm and/or Tn tail shifts significantly.

To detect movement of Tm, FRET has been applied. Cys-190 on Tm and Cys-374 or Lys-61 on actin were first used as probe sites (*16–18*). However, FRET did not detect any significant movement of Tm such as the steric blocking model predicted. On the other hand, Tao *et al*. (*17*) suggested that the Tm-bound donor (Cys-190) and the actin-bound acceptor (Cys-374) might be located relative to each other so that the movement of Tm with respect to the grooves of actin produces no net change in the extent of energy transfer. However, such donor-acceptor locations are restricted to a narrow area, when Tm movement is only azimuthal. That is, the donor position on Tm moves on a circle with the acceptor position as its center, as viewed through the cross-section of a thin filament. If the donor and acceptor probes could be attached at positions on the outside of its restricted narrow area, large change in the transfer efficiency could be expected when Tm moves on the actin filament. Then, several positions, Cys-374, Lys-61, Gln-41, and the nucleotide-binding site on actin and Cys-190 and Cys-87 on Tm were labeled (*22*). FRET between these sites on actin and Tm detected no significant change in the transfer efficiency upon removal of Ca^{2+} ions. The results strongly suggested that Tm does not move on the F-actin filament, since it is difficult to find Tm movement on a circle with these different acceptor positions as the center at the same time. On the other hand, a three-state model (blocked, closed, and open states) has been proposed from kinetic measurements, and the steric model has been coupled with this three-state model. Structural studies of the low angle X-ray diffraction of muscle thin filament and 3D-EM of reconstituted thin filaments suggested three positions of Tm on the actin filament. However, FRET did not detect any change of transfer efficiency not only for Ca^{2+}-induced but also for S1-induced Tm movement. So it is more difficult to find three different positions (blocked, closed, and open) than two different positions (on and off) for the donor probe on Tm all of which are equally distant from acceptors on actin. Recently, Bacchiocchi and Lehrer (*42*) reported that a small change in the transfer efficiency could be interpreted as reflecting a large change in the azimuthal position of Tm on an actin filament from the analysis of phase/modulation *vs*. frequency data, suggesting that Tm rolls on the surface of actin. This is because without assuming rolling of Tm on the actin surface, Tm would have to detach from actin in order to find two positions ($+Ca^{2+}$ and $-Ca^{2+}$) of donor on Tm that are equidistant from the acceptor positions on actin. In their experiments, two donor molecules attached to Cys-190 on two α-chains of Tm were used for analysis. Positions 87, 190, 237, 245, 247 and 252 of Tm are designed to locate at positions c, a, f, g, b and g, respectively in the seven-times repeated α-helical coiled-coil structure of Tm. The donor

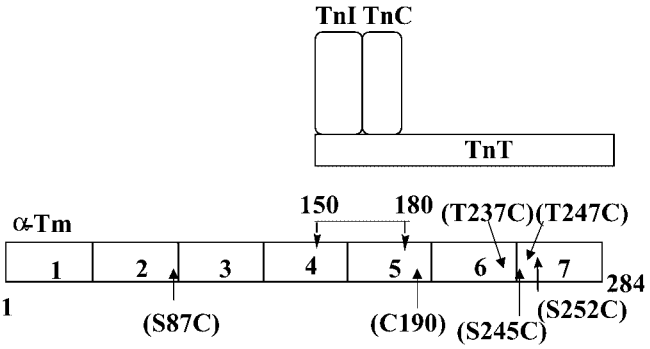

Fig. 7. **A schematic representation of the troponin-tropomyosin complex with the donor-labeling sites on Tm.** The Tm molecule contains seven quasiequivalent regions, each of which contains a pair of putative actin-binding motifs. X-ray analysis of co-crystals of tropomyosin and troponin revealed that the globular parts of the troponin complex binds tropomyosin near residues 150–180 (*46*).

probes at these sites project at different angles to each other on the Tm surface. In this case, it is also difficult to find two rolling positions (+Ca^{2+} and –Ca^{2+}) of Tm without changing the distance between donor and acceptor probes. Moreover, if rolling of Tm on the actin surface occurs during inhibition (*42*), the attachment of a large molecule such as fluorescent dye on the surface of Tm may strongly affect the regulatory activity of Tm. But the attachment of a donor probe did not impair the regulatory ability of Tm (Fig. 1).

Narita *et al*. showed that the N-terminal region of Tm does not move much (*13*) and pointed out that the positions 87 and 190 on Tm previously used as labeling sites are located in this region, which is rather insensitive to Ca^{2+}. We therefore generated four mutants, each of which has a unique cysteine residue in the C-terminal one-third (Fig. 7). However, FRET measurements between probes attached to these positions of Tm and Cys-374 or Gln-41 of actin did not show any significant change in the transfer efficiency by Ca^{2+}- or S1-induced conformational change of thin filaments.

Graceffa (*37*) suggested that the skeletal muscle αα-Tm has a donor symmetrically protruding from either side of the Tm coiled-coil and consequently the energy transfer from such a "broad" donor may not have the resolution necessary to clearly detect net changes in the distance. We therefore mixed labeled αα-Tm homodimer with non-labeled ββ-Tm homodimer to produce singly labeled αβ-Tm heterodimer according to their methods. However, FRET measurements with singly labeled αβ-Tm showed no change in the transfer efficiency during Ca^{2+}- or S1-induced conformational change of thin filaments (Table 3). On the other hand, Ca^{2+}- or S1-binding to the regulated thin filament induces a change in the rotational motions of probes attached to actin or Tm. This may affect the orientation factor, the mutual orientation of the dipoles of donor and acceptor probes. The transfer efficiency strongly depends on the value of the orientation factor, but in the present FRET measurements, the transfer efficiency between probes on actin and Tm did not depend on the states of the thin filament. The rotational relaxation times of probes attached to Cys-374 on F-actin (200–400 ns) (*43*) or Cys-190 on Tm in reconstituted thin filaments (several components in the range 7–4,000 ns) (*44*) are much shorter than the values calculated for a whole molecule. Even though the rotational relaxation times were affected by Ca^{2+}- or S1-binding, directions of transition moments of probes were randomized due to segmental motions in an equilibrium state. Consequently, the average of relative orientations of the transition dipoles attached to actin and Tm did not depend on Ca^{2+}- or S1-binding to the thin filament.

We measured time-resolved FRET by use of stopped-flow methods in order to detect a transient change in the distance during Tm movement. Since Tn is a Ca^{2+} sensor, it is reasonable to assume that Tm moves simultaneously with or after Tn movement upon Ca^{2+} binding to or detaching from TnC. Figure 6 clearly shows the TnI movement from +Ca^{2+} to –Ca^{2+} states or vice visa. However, we did not detect any change in the transfer efficiency between probes attached to Tm and actin in the time range when Tm might move on actin filaments. Although the labeling positions of the donor probe cover nearly the whole of Tm, and the labeling positions of the acceptor probes are spread over actin, FRET did not detect any trace of Tm movement from +Ca^{2+} to –Ca^{2+} or vice versa. Instead of Tm movement, FRET has detected significant extents of movement of TnI (*18–21*, *24*, *25*) and TnT (*26*). Furthermore, these TnI and TnT movements correspond well to the three states of thin filaments (*25–27*). Therefore, it is unrealistic to consider that only Tm movement is invisible by FRET.

In previous analyses of 3D-EM using helical symmetry, the contributions from Tn and Tm were averaged over the structure of actin filament. By analyzing electron cryo-micrographs without imposing helical symmetry, Narita *et al*. (*13*) explicitly assessed the contribution of Tn to global helical projections. They showed that the globular portion of Tn (Tn head) changes its conformation and moves towards the outer domain of actin, covering the N- and C-terminals of actin. Further, they showed that the tail region of Tn (Tn tail) and/or the C-terminal region of Tm move towards the outer domain of actin, but that the N-terminal region of Tm does not move significantly. By taking into account this Tn movement, the extent of the shift of Tm was estimated to be much smaller than in previous analysis. However, the resolution of the reconstruction was not high enough to distinguish precisely the contribution of the Tn tail (N-terminal region of TnT) and the C-terminal one-third of Tm. TnT is an elongated molecule and binds to the C-terminal half of Tm (Fig. 7). The large shift due to the Tn tail and/or C-terminal region of Tm observed by Narita *et al*. (*13*) may be better explained by taking into account a greater mass movement of the Tn head and tail regions without Tm movement, as observed by FRET measurements. Recently, the crystal structure of the core domain of troponin has been elucidated (*45*). By use of the atomic structures in analyses of conformational changes of thin filaments from the data of X-ray diffraction and 3D-EM, it is expected to get more precise images of the conformational change of the muscle thin filament. Thin filament structures with higher resolution are required to reconcile the apparent inconsistency between FRET and 3D-EM observations.

We thank The Food Research and Development Laboratories of Ajinomoto Co. for the generous gift of microbial transglutaminase, and Prof. Ikunobu Muramatsu of Fukui University for kindly providing rabbit hearts. This study was performed through the Special Coordination Funds of the Ministry of Education, Culture, Sports, Science and Technology of Japan.

REFERENCES

1. Ebashi, S., Endo, M., and Ohtsuki, I. (1969) Control of muscle contraction. *Q. Rev. Biophys.* **2**, 351–384
2. Ohtsuki, I. and Wakabayashi, T. (1972) Optical diffraction studies on the structure of troponin-tropomyosin-actin paracrystals. *J. Biochem.* **72**, 369–377
3. Ohtsuki, I., Maruyama, K., and Ebashi, S. (1986) regulatory and cytoskeletal proteins of vertebrate skeletal muscle. *Adv. Protein Chem.* **38**, 1–67
4. Farah, C.S. and Reinach, F.C. (1995) The troponin complex and regulation of muscle contraciton. *FASEB J.*, **9**, 755–767
5. Gordon, A.M., Homsher, E., and Regnier, M. (2000) Regulation of contraction in striated muscle. *Physiol. Rev.* **80**, 853–924
6. Huxley, H.E. (1972) Structural changes in the actin and myosin containing filaments during contraction. *Cold Spring Harbor Symp. Quant. Biol.* **37**, 361–376
7. Haselgrove, J. (1972) X-ray evidence for a conformational change in the actin containing filaments of vertebrate striated muscle.*Cold Spring Harbor Symp. Quant. Biol.* **37**, 341–352
8. Mckillop, D.F. and Geeves, M.A. (1993) Regulation of the interaction between actin and myosin subfragment 1: evidence for three states of the thin filament. *Biophys. J.* **65**, 693–701
9. Geeves, M.A. and Lehrer, S.S. (1994) Dynamics of the muscle thin filament regulatory switch: the size of the cooperative unit. *Biophys. J.* **67**, 273–282
10. Lehrer, S.S. and Geeves, M.A. (1998) The muscle thin filament as a classical cooperative/allosteric regulatory system. *J. Mol. Biol.* **277**, 1081–1089
11. Holmes, K.C. (1995) The actomyosin interaction and its control by tropomyosin. *Biophys. J.* **68**, 2s–7s
12. Vibert, P., Craig, R., and Lehman, W. (1997) Steric-model for activation of muscle thin filamenents. *J. Mol. Biol.* **266**, 8–14
13. Narita, A., Yasunaga, T., Ishikawa, T., Mayanagi, K., and Wakabayashi, T. (2001) Ca^{2+}-induced switching of troponin and tropomyosin on actin filaments as revealed by electron cryomicroscopy. *J. Mol. Biol.* **308**, 241–261
14. Miki, M., O'Donoghue, S.I., and dos Remedios, C.G. (1992) Structure of actin observed by fluorescence resonance energy transfer spectroscopy. *J. Muscle Res. Cell Motil.* **13**, 132–145
15. dos Remedios, C.G. and Moens, P.D. (1995) Fluorescence resonance energy transfer spectroscopy is a reliable "ruler" for measuring structural changes in proteins: Dispelling the problem of the unknown orientation factor. *J. Struct. Biol.* **115**, 175–185
16. Miki, M. and Mihashi, K. (1979) Conformational changes of reconstituted thin filament under the influence of Ca^{2+} ion-fluorescence energy transfer and anisotropy decay measurements. *Seibutsu-Butsuri* **19**, 135–140 (in Japanese)
17. Tao, T., Lamkin, M., and Lehrer, S.S. (1983) Excitation energy transfer studies of the proximity between tropomyosin and actin in reconstituted skeletal muscle thin filaments. *Biochemistry* **22**, 3059–3066
18. Miki, M. (1990) Resonance energy transfer between points in a reconstituted skeletal muscle thin filament: A conformational change of the thin filament in response to a change in Ca^{2+} concentration. *Eur. J. Biochem.* **187**, 155–162
19. Tao, T., Gong, B.J., and Leavis, P.C. (1990) Calcium-induced movement of troponin-I relative to actin in skeletal muscle thin filaments. *Science* **247**, 1339–1341
20. Miki, M. and Iio, T. (1993) Kinetics of structural changes of reconstituted skeletal muscle thin filaments observed by fluorescence resonance energy transfer. *J. Biol. Chem.* **268**, 7101–7106
21. Miki, M., Kobayashi, T., Kimura, H., Hagiwara, A., Hai, H., and Maéda, Y. (1998) Ca^{2+} -induced distance change between points on actin and troponin in skeletal muscle thin filaments estimated by fluorescence energy transfer spectroscopy. *J. Biochem.* **123**, 324–331
22. Miki, M., Miura, T., Sano, K., Kimura, H., Kondo, H., Ishida, H., and Maéda, Y. (1998) Fluorescence resonance energy transfer between points on tropomyosin and actin in skeletal muscle thin filaments: Does tropomyosin move? *J. Biochem.* **123**, 1104–1111
23. Miki, M. (2002) Structural changes between regulatory proteins and actin: A regulation model by tropomyosin-troponin based on FRET measurements in *Molecular Interactions of Actin*, (Thomas, D.D. and dos Remedios, C.G., eds.) Vol. **2**, pp. 191–203, Springer Verlag, Heidelberg
24. Kobayashi, T., Kobayashi, M., and Collins, J.H. (2001) Ca^{2+}-dependent, myosin subfragment 1-induced proximity changes between actin and the inhibitory region of troponin I. *Biochim. Biophys. Acta* **1549**, 148–154
25. Hai, H., Sano, K., Maeda, K., Maéda Y. and Miki, M. (2002) Ca^{2+}-induced conformational change of reconstituted skeletal muscle thin filaments with an internal deletion mutant D234-tropomyosin observed by fluorescence energy transfer spectroscopy: Structural evidence for three states of thin filament. *J. Biochem.* **131**, 407–418
26. Kimura, C., Maeda, K., Maeda, Y., and Miki, M. (2002) Ca^{2+}- and S1-induced movement of troponin T on reconstituted skeletal muscle thin filaments observed by fluorescence energy transfer spectroscopy. *J. Biochem.* **132**, 93–102.
27. Kimura, C., Maeda, K., Hai, H., and Miki, M. (2002) Ca^{2+}- and S1-induced movement of troponin T on mutant thin filaments reconstituted with functionally deficient mutant tropomyosin. *J. Biochem.* **132**, 345–352.
28. Nonaka, M., Sakamoto, H., Toiguchi, S., Kawajiri, H., Soeda, T., and Motoki, M. (1992) Sodium caseinate and skim milk gels formed by incubation with microbial transglutaminase. *J. Food Sci.* **57**, 1214–1241
29. Kim, E., Motoki, M., Seguro, K., Muhlrad, A., and Reisler, E. (1995) Conformational changes in subdomain 2 of G-actin: Fluorescence probing by dansyl ethylenediamine attached to Gln-41. *Biophys. J.* **69**, 2024–2032
30. Kluwe, L., Maeda, K., Miegel, A., Fujita-Becker, S., Maéda, Y., Talbo, G., Houthaeve, T., and Kellner, R. (1995) Rabbit skeletal muscle αα-tropomyosin expressed in baculovirus-infected insect cells possesses the authentic N-terminus structure and functions. *J. Muscle Res. Cell Motil.* **16**, 103–110
31. Monteiro, P.B., Lataro, C., Ferro, J.A., and Reinach, F.C. (1994) Functional α-tropomyosin produced in *Escherichia coli*. *J. Biol.Chem.* **269**, 10461–10466
32. Kunkel, T.A. (1985) Rapid and efficient site-specific mutagenesis without phenotypic selection. *Proc. Natl Acad. Sci. USA* **82**, 488–492
33. Miegel, A., Sano, K., Yamamoto, K., Maeda, K., Maéda, Y., Taniguchi, H., Yao, M., and Wakatsuki, S. (1996) Production and crystallization of lobster muscle tropomyosin expressed in Sf9 cells. *FEBS Lett.* **394**, 201–205.
34. Lorand, L., Parameswaran, K.N., Velasco, P.T., Hsu, L.K.-H., and Siefring, G.E., Jr. (1983) New colored and fluorescent amine substrates for activated fibrin stabilizing factor (Factor XIIIa) and for transglutaminase. *Anal. Biochem.* **131**, 419–425
35. Hudson, E.N. and Weber, G. (1973) Synthesis and characterization of two fluorescent sulfhydryl reagents. *Biochemistry* **12**, 4154–4161
36. Graceffa, P. (1992) Heat-treated smooth muscle tropomyosin. *Biochim. Biophys. Acta* **1120**, 205–207
37. Graceffa, P. (1999) Movement of smooth muscle tropomyosin by myosin heads. *Biochemistry* **38**, 11984–11992.
38. Scott, T.G., Spencer, R.D., Leonard, N.G., and Weber, G. (1970) Emission properties of NADH. Studies of fluorescence life-

times and quantum efficiencies of NADH, AcPyADH, and simplified synthetic models. *J. Amer. Chem. Soc.* **92**, 687–695
39. Laemmli, U.K. (1970) Cleavage of structural proteins during the assembly of the head of bacteriophage T4. *Nature (Lond.)* **227**, 680–685
40. Tausky, H.H. and Shorr, E. (1953) A microcolorimetric method for the determination of inorganic phosphorus. *J. Biol. Chem.* **202**, 675–685
41. Squire, J.M. and Morris, E.P. (1998) A new look at thin filament regulation in vertebrate skeletal muscle. *FASEB J.* **12**, 761–771
42. Bacchiocchi, C. and Lehrer, S.S. (2001) Ca^{2+}-induced movement of tropomyosin in skeletal muscle thin filaments observed by multi-site FRET. *Biophys. J.* **82**, 1524–1536
43. Miki, M., Wahl, Ph., and Auchet, J.-C. (1982) Fluorescence anisotropy of labeled F-actin: Influence of divalent cations on the interaction between F-actin and myosin heads. *Biochemistry* **21**, 3661–3665
44. Wahl, Ph., Tawada, K., and Auchet, J.-C. (1979) Study of tropomyosin labelled with a fluorescent probe by pulse fluorimetry in polarized light: Interaction of that protein with troponin and actin. *Eur. J. Biochem.* **88**, 421–424
45. Takeda, S., Yamashita, A., Maeda, K., and Maéda, Y. (2003) Structure of the core domain of human cardiac troponin in the Ca^{2+}-saturated form. *Nature* **424**, 35–41
46. White, S.P., Cohen, C., and Phillips, G.N., Jr (1987) Structure of co-crystals of tropomyosin and troponin. *Nature* **325**, 826–828